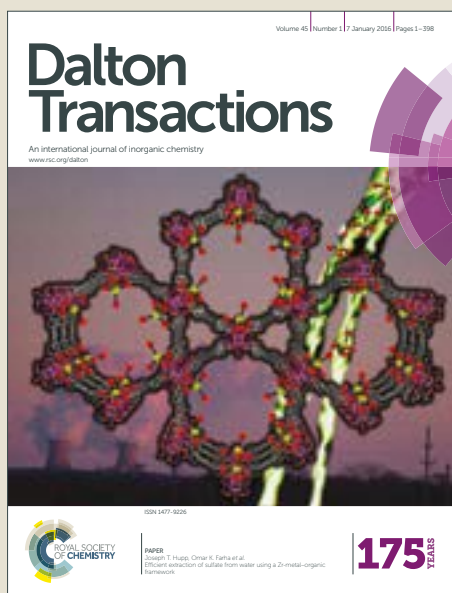


# Dalton Transactions

Accepted Manuscript



This article can be cited before page numbers have been issued, to do this please use: G. Mani, V. K. JHA, Y. R. Davuluri and A. Anoop, *Dalton Trans.*, 2017, DOI: 10.1039/C6DT04458A.



This is an Accepted Manuscript, which has been through the Royal Society of Chemistry peer review process and has been accepted for publication.

Accepted Manuscripts are published online shortly after acceptance, before technical editing, formatting and proof reading. Using this free service, authors can make their results available to the community, in citable form, before we publish the edited article. We will replace this Accepted Manuscript with the edited and formatted Advance Article as soon as it is available.

You can find more information about Accepted Manuscripts in the [author guidelines](#).

Please note that technical editing may introduce minor changes to the text and/or graphics, which may alter content. The journal's standard [Terms & Conditions](#) and the ethical guidelines, outlined in our [author and reviewer resource centre](#), still apply. In no event shall the Royal Society of Chemistry be held responsible for any errors or omissions in this Accepted Manuscript or any consequences arising from the use of any information it contains.



## Journal Name

## ARTICLE

Received 00th January  
20xx,

## The Pyrrole Ring $\eta^2$ -Hapticity Bridged Binuclear Tricarbonyl Mo(0) and W(0) Complexes: Catalysis of Regioselective Hydroamination Reactions and DFT Calculations

Accepted 00th January 20xx

Vikesh Kumar Jha, Ganesan Mani,<sup>\*,a</sup> Yogeswara Rao Davuluri and Anakuthil Anoop

DOI: 10.1039/x0xx00000x

www.rsc.org/

Following the report of ferrocene structure, metal complexes containing the heteroatom substituted cyclopentadienyl (Cp) analogue, that is,  $\eta^5$  pyrrolyl ligand, have been reported. While the Cp ligand continues to be a favorite ligand in organometallics, the transition metal chemistry of pyrrolyl ligand is still in the developing stage. In view of this, we carried out the reaction between the multidentate ligand 2,3,4,5-tetrakis(3,5-dimethylpyrazolylmethyl)pyrrole (**LH**) and Mo(CO)<sub>6</sub> or [W(CO)<sub>3</sub>(CH<sub>3</sub>CN)<sub>3</sub>] and isolated two new binuclear tricarbonyl Mo(0) and W(0) complexes, [Mo<sub>2</sub>(CO)<sub>6</sub>( $\mu$ - $\eta^2$ : $\eta^2$ -**LH**- $\kappa^4$ N)] **1** and [W<sub>2</sub>(CO)<sub>6</sub>( $\mu$ - $\eta^2$ : $\eta^2$ -**LH**- $\kappa^4$ N)] **2**. Their X-ray structural analyses showed the metal centers are bridged by the double bonds of the central pyrrole ring ( $\mu$ - $\eta^2$ : $\eta^2$ ), a rarely observed coordination mode. Interestingly, complex **1** is a catalyst precursor for the hydroamination reactions of phenylacetylene with a series of secondary amines at room temperature offering the regioselectively formed anti-Markovnikov product in excellent yields. In addition, DFT calculations were performed to understand the bonding nature of the pyrrole ring in **1** and **2** and to estimate the energy of six different conformations of **LH**.

### Introduction

Since the report of the X-ray structure analysis of ferrocene,<sup>1</sup> cyclopentadienyl ligands played a major role in the development of the transition metal organometallic chemistry. Cyclopentadienyls adopts not only the ubiquitous  $\eta^5$  coordination mode, but also bonding modes such as  $\sigma$ ,<sup>2</sup>  $\eta^3$ ,<sup>3</sup> and  $\eta^4$ .<sup>4</sup> Conversely, metal complexes containing the isoelectronic 6 electron donor pyrrolyl ligand azacyclopentadienyls have not been extensively studied, though a large progress has been done.<sup>5</sup> In addition to their most common bridging mode  $\kappa$ N- $\eta^5$  found in transition<sup>6</sup> and lanthanide metals,<sup>7</sup> sandwich complexes containing one<sup>8</sup> or two<sup>9</sup>  $\eta^5$  pyrrolyl and half sandwich<sup>10</sup> complexes have been reported. It also displayed bonding modes such as  $\eta^3$ ,<sup>11</sup> and bridging  $\kappa$ N- $\eta^2$ .<sup>12</sup> Further, Floriani and co-workers have reported the lithium complex of *meso*-octaethylcalix[4]pyrrole in which the pyrrole ring adopts the  $\eta^2$  bonding mode.<sup>13</sup>

We recently reported the direct synthesis of multidentate ligand, 2,3,4,5-tetrakis(3,5-dimethylpyrazolylmethyl)pyrrole (**LH**). It is a source of azacyclopentadienyl anion containing four neutral pyrazole nitrogen donors upon the deprotonation of the pyrrole NH, and its binuclear and multinuclear

complexes have been reported.<sup>14</sup> As a continuation of our work on this ligand, herein we report the synthesis, structural characterization of molybdenum(0) and tungsten(0) tricarbonyl complexes bearing **LH** in which the pyrrole ring possesses the new bridging coordination mode. We also report the catalysis of hydroamination reactions of phenylacetylene with secondary amines using the **LH** molybdenum complex and the DFT calculations for both complexes and ligand.

### Results and discussion

#### Synthesis and Structure of Mo and W Complexes

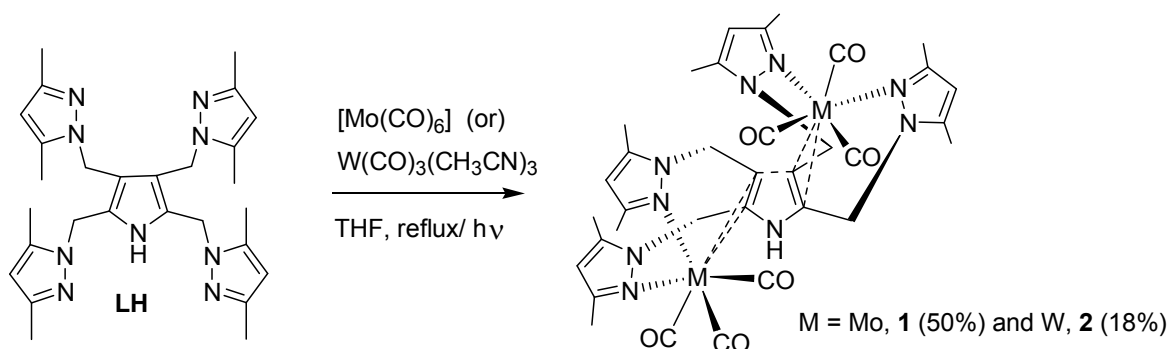
**LH** reacts with two equiv of Mo(CO)<sub>6</sub> in THF under reflux conditions or photolysis to give the binuclear Mo(0) carbonyl complex **1** containing one neutral ligand **LH** in about 50% yield (Scheme 1). The <sup>1</sup>H NMR spectrum of complex **1** in CDCl<sub>3</sub> showed well-resolved resonances, indicating the rigid structure of **1** maintained in solution. The pyrrolic NH resonance appears at  $\delta$  9.26 ppm as a broad singlet, which is shifted downfield as compared to that of the free ligand. The diastereotopic methylene protons of **LH** in **1** appears as two well separated AB pattern with  $J(\text{H}_A\text{H}_B) = 15.2$  Hz. This is in contrast to the two broad singlets observed for the free ligand. In addition, four singlet resonances corresponding to the four different methyl groups were observed and their integrated intensity values are in accord with the structure. The FT-IR spectrum showed strong  $\nu(\text{CO})$  stretching frequency bands at 1909, 1793 and 1778 cm<sup>-1</sup>, suggesting the presence of three terminal COs.

<sup>a</sup> Department of Chemistry, Indian Institute of Technology – Kharagpur, Kharagpur, West Bengal, India 721 302, Fax: +91 3222 282252, E-mail: gmani@chem.iitkgp.ernet.in.

Electronic Supplementary Information (ESI) available: Experimental procedure, NMR, IR spectra, crystallographic data (CIF) and DFT calculations data and coordinates. CCDC 1518990-1518991, See DOI: 10.1039/x0xx00000x

## Journal Name

## ARTICLE

Scheme 1. Synthesis of the Mo(0) **1** and W(0) **2** complexes of LH.Table 1. Selected bond lengths (Å) and angles (deg) for complex **1** and **2**.

Mo complex <b>1</b>				W complex <b>2</b>			
C(1)-Mo	1.942(2)	C(1)-Mo-N(5)	178.61(8)	C(1)-W	1.936(3)	C(1)-W-N(5)	177.80(12)
C(2)-Mo	1.950(3)	C(2)-Mo-N(3)	169.52(8)	C(2)-W	1.950(4)	C(2)-W-N(3)	169.52(12)
C(3)-Mo	1.940(2)	C(3)-Mo-C(1)	84.70(9)	C(3)-W	1.949(4)	C(1)-W-C(3)	85.39(13)
N(3)-Mo	2.2805(19)	C(3)-Mo-N(5)	96.10(8)	N(3)-W	2.248(3)	C(3)-W-N(5)	95.11(12)
N(5)-Mo	2.2659(18)	N(5)-Mo-N(3)	83.63(6)	N(5)-W	2.247(3)	N(5)-W-N(3)	83.37(10)
C(4)-Mo	2.614(2)	C(1)-Mo-N(3)	95.12(8)	C(4)-W	2.567(3)	C(1)-W-N(3)	94.44(11)
C(5)-Mo	2.563(2)			C(5)-W	2.511(3)		

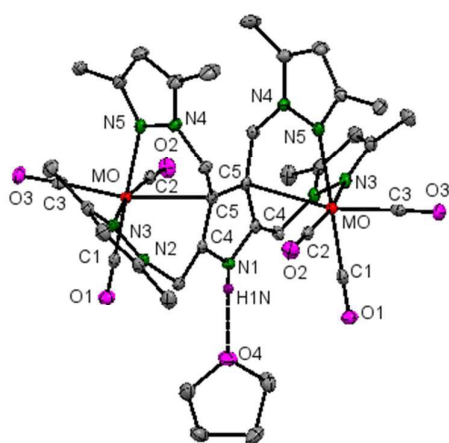
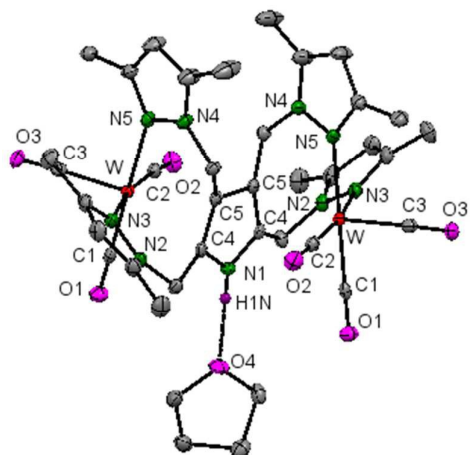


Figure 1. ORTEP diagram (50% thermal ellipsoids) of complex **1**. Most hydrogen atoms are omitted for clarity. N1<sup>⋯</sup>O4 2.782(4) Å, H1N<sup>⋯</sup>O4 2.05(4) Å, N1–H1N<sup>⋯</sup>O4 180.0°. Symmetry transformations used to generate equivalent atoms: (i)  $-x+2, y, -z+1/2$ , (ii)  $-x+3, y, -z+1/2$ , (iii)  $x-1/2, y-1/2, z$ .

The X-ray structure of complex **1** is given in Figure 1, and selected metric parameters and refinement data are given in Table 1 and Table 3, respectively. The molecule crystallizes in the centrosymmetric space group  $C2/c$  and the asymmetric

unit constitutes one half of the molecule and thf. The X-ray structure revealed that the molecule consists of two 'Mo(CO)<sub>3</sub>' units bridged by one neutral ligand LH. Each Mo(CO)<sub>3</sub> unit is coordinated by two pyrazolyl nitrogens, creating a nine-membered ring having a 'tub' shape with a deep cavity. This conformation facilitates the pyrrole ring to bind to the metal atoms via its double bond π-electrons and to bridge the two metal centers on either side, representing a rarely observed coordination mode μ-η<sup>2</sup>:η<sup>2</sup> of the pyrrole ring. If the pyrrole ring π-coordination is treated as the tail of a scorpion, then the coordination mode of ligand LH is reminiscent of the famous polypyrazolylborate scorpionate ligand<sup>15</sup> and indicates its flexibility. The resulting coordination environment causes the pyrazole moieties as well as the two Mo(CO)<sub>3</sub> units lie above and below the pyrrole ring plan, which is similar to the conformation LH adopted in the structures of reported binuclear Pd(II) and Ag(I) complexes.<sup>14</sup> The geometry around the molybdenum atom is a distorted octahedron with C1–Mo–N5 angle of 178.61(8)° being larger than the C2–Mo–N3 angle value of 169.52(8)° probably because of steric hindrance of two pyrazole methyl groups and the constraint, created by the presence of one rigid methylene group between the pyrazole and pyrrole rings, with which the pyrazolyl nitrogens coordinate. This steric effect causes the

pyrrole ring C–Mo  $\pi$ -bond distances 2.614(2) Å and 2.563(2) Å to be longer than those found in [Mo(CO)<sub>4</sub>(COD)] (2.462(6) to 2.497(6) Å),<sup>16</sup> indicating that they are relatively weaker bonds. In addition, this is reflected in the Mo–CO distances which are almost identical (1.940(2) Å, 1.942(2) Å and 1.950(3) Å). Ideally Mo–C<sub>3</sub>O distance lies trans to the pyrrole  $\pi$ -bond is supposed to be longer than the other two distances (Mo–C<sub>1</sub>O and Mo–C<sub>2</sub>O) lie trans to the  $\sigma$  donor pyrazole nitrogen atoms because usually simple alkenes are weaker  $\pi$ -acceptors than CO. Nevertheless, the pyrrole ring C<sub>4</sub>–C<sub>5</sub> double bond distance is elongated to 1.396(3) Å as compared to the corresponding C–C distance (1.359(6) Å) found in the structure of 2,5-bis(3,5-dimethylpyrazolylmethyl)pyrrole.<sup>17</sup> Eventually, the substitution of three COs in Mo(CO)<sub>6</sub> by three donors results in the formation of complex containing three different Mo–CO groups. In addition, the two pyrazole N–Mo bond distances (N3–Mo = 2.2805(19) Å and N5–Mo = 2.2659(18) Å) are slightly different. The pyrrole ring NH is strongly hydrogen bonded to the lattice THF molecule as shown by the distance and angle, and as a result the NH hydrogen atom was located in the X-ray structure.



**Figure 2.** ORTEP diagram (50% thermal ellipsoids) of complex **2**. Most hydrogen atoms are omitted for clarity. N1 $\cdots$ O4 2.779(5) Å, H1N $\cdots$ O4 1.95(6) Å, N1–H1N $\cdots$ O4 180.0°. Symmetry transformations used to generate equivalent atoms:  $-x, y, -z + 1/2$ .

The analogous tungsten complex **2** was obtained from the reaction of [W(CO)<sub>3</sub>(CH<sub>3</sub>CN)<sub>3</sub>] with **LH** under reflux conditions in poor yield. The <sup>1</sup>H NMR spectrum is similar to that of the molybdenum complex **1**, suggesting a similar structure. The presence of terminal COs is shown by the FT-IR spectrum featuring strong  $\nu$ (CO) bands at 1899, 1791 and 1773 cm<sup>-1</sup>, which are lower than those for complex **1**. Complex **2** was crystallized from the same solvent, THF/petroleum ether, which was used for complex **1** and the unit cell parameters show that the crystal lattice of **2** is isomorphous to **1**. The X-ray structure of **2** is given in Figure 2; it closely resembles the structure of complex **1**. However, its metric parameters are slightly different owing to their covalent radii difference. The bridging pyrrole ring  $\eta^2$  hapticity found in this structure possesses the W–C distances of 2.567(3) Å and 2.511(3) Å, which are shorter and hence stronger than those in the Mo

complex **1** because the covalent radius<sup>18</sup> of W (1.62(7) Å) is greater than that of Mo (1.54(5) Å). However, these W–C distances are longer than those found in the reported alkene bound W complexes such as [W(CO)<sub>3</sub>(P(OMe)<sub>3</sub>)(COD)] (2.395(5) to 2.424(6) Å),<sup>19</sup> [(Tp'W(CO)<sub>2</sub>)(C<sub>2</sub>S<sub>2</sub>){(Cp)Ru(PPh<sub>3</sub>)}] (2.066(7) Å and 2.049(6) Å),<sup>20</sup> [( $\eta^4$ -norbornadiene)W(CO)<sub>4</sub>] (2.403(6) to 2.419(5) Å)<sup>21</sup> and [W(CO)<sub>5</sub>( $\eta^2$ -C<sub>7</sub>H<sub>10</sub>)] (2.497(16) and 2.510(15) Å).<sup>22</sup> As found for **1**, the pyrrole ring C<sub>4</sub>–C<sub>5</sub> double bond distance (1.404(5) Å) is also longer than that (1.359(6) Å) found in the structure of 2,5-bis(3,5-dimethylpyrazolylmethyl)pyrrole. In addition, the W–C<sub>3</sub>O distance (1.949(4) Å) trans to the pyrrole  $\pi$ -bond is slightly longer than the Mo–C<sub>3</sub>O distance in **1** and the C<sub>3</sub>O<sub>3</sub> competes for the metal back bonding with the pyrrole ring  $\pi$  bond.

## Hydroamination Reactions

The hydroamination of C–C multiple bonds is an atom efficient process and provides bulk and fine chemicals, and versatile intermediates for further reactions. A large number of catalysts based on metals across the periodic table have been known for mediating these reactions.<sup>23,24,25,26,27,28</sup> Hydroamination reactions involving ammonia as the amine partner,<sup>29,30</sup> and energy efficient room temperature catalysis<sup>31</sup> have also been reported. Nevertheless, the field continues to attract the attention of researchers because of the challenges in developing catalysts for selective anti-Markovnikov hydroamination of aliphatic olefin,<sup>32</sup> and regioselective addition of ammonia to olefins.<sup>33</sup> In this industrially important research field, McDonald et. al. reported the [Mo(CO)<sub>5</sub>(Et<sub>3</sub>N)] catalyzed intramolecular hydroamination of alkynylamines.<sup>34</sup> Recently, Szymańska-Buzar and co-workers have reported the first hydroamination reaction of terminal alkynes in the presence of tungsten carbonyl complex [W(CO)<sub>4</sub>(piperidine)<sub>2</sub>].<sup>35</sup>

We found complex **1** catalyzes the hydroamination of terminal alkyne PhCCH with a series of secondary amines; the optimized reaction conditions and yields are given in Table 2. In cases of morpholine and piperazine, the reactions go cleanly at room temperature with very high yields of the stereo- and regioselectively formed anti-Markovnikov product, *E*-isomer, in the presence of ~0.4 mol% of the pre-catalyst **1**. Products were obtained in almost pure form by just removing the volatiles from the resulting reaction mixture. However, an elevated temperature is required to obtain the best yields of the anti-Markovnikov products formed in the piperidine and pyrrolidine reactions, as shown in Table 2. The reactions with these two amines at room temperature are slow and their <sup>1</sup>H NMR spectra showed unreacted starting materials. To test the efficiency of the catalytic activity of complex **1**, the reaction between PhCCH and morpholine or phenylpiperazine was carried out in the presence of Mo(CO)<sub>6</sub> (1 mol%) as catalyst under reflux conditions and we found that a mixture of products including the anti-Markovnikov (20%)<sup>36</sup> and the phenylacetylene dimer were formed. In addition, the starting materials were not consumed, as shown by their <sup>1</sup>H NMR and GCMS data. Besides, there is no product formed for the same

## ARTICLE

**Table 2.** Hydroamination of PhCCH with secondary amines catalyzed by the Mo complex **1**.

$\text{Ph}-\text{C}\equiv\text{C}-\text{H} + \text{R}_2\text{NH} \xrightarrow[\text{No solvent, r.t.}]{\text{Complex 1}} \text{Ph}-\text{CH}=\text{CH}-\text{NR}_2$					
Amine (PhCCH : amine)	Product	1, mol%	t, h	T, °C	Yield (%)
1 		0.4	96	28	92
2 		0.4	96	28	90
3 		0.43	96	28	89
4 		0.41	5	80	70
5 		0.42	3	80	36

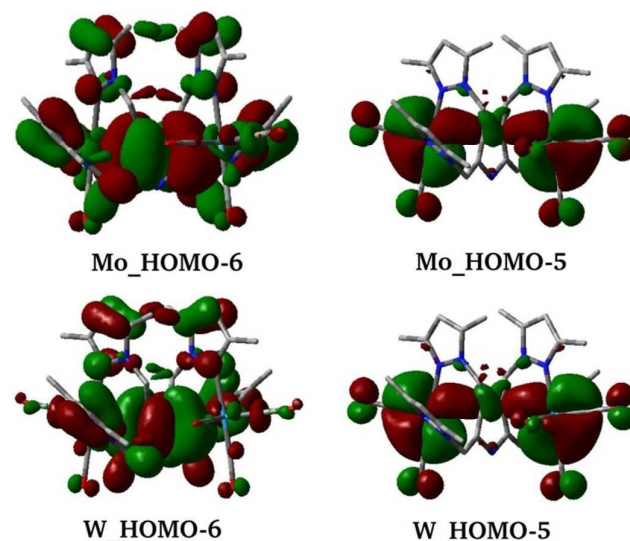
reaction at room temperature for 12 h. This emphasizes the importance of the role played by ligand **LH** coordinated to the Mo atom in complex **1**. Further, the observed catalytic activity can be ascribed to the binuclear nature of complex **1**. However, complex **1** failed to selectively yield the desired hydroaminated product even under reflux conditions for alkynes such as 1-hexyne and 1-phenyl-1-propyne and for styrene, which gave a mixture of products. This indicates complex **1** is selective toward the hydroamination of phenylacetylene with the examined secondary amines to give the anti-Markovnikov product. Furthermore, complex **2** also

catalyzes the formation of anti-Markovnikov **3** slowly at room temperature.

In an attempt to understand the mechanism of the catalysis, the reaction was monitored by  $^1\text{H}$  NMR method. The  $^1\text{H}$  NMR spectrum of complex **1** with one equiv of PhCCH in  $\text{CD}_2\text{Cl}_2$  showed no change in the spectral pattern. However, the spectrum recorded after 24 h for the same solution in the presence of one equiv of morpholine showed the disappearance of the pyrrolic NH proton and appearance of two singlets at  $\delta$  4.82 and 5.02 ppm, which is for the free ligand. In addition, the spectrum also showed the presence of the intact complex **1**, starting materials and negligible amount of the product. This indicates the catalyst decomposes via the deprotonation of the pyrrole NH proton and the product formation is very slow in  $\text{CH}_2\text{Cl}_2$  at room temp. On the other hand, the  $^1\text{H}$  NMR spectrum recorded for a mixture of PhCCH, morpholine and **1** kept at room temp for 3 days, giving solid and then dissolved in  $\text{C}_6\text{D}_6$  showed the disappearance of starting materials and cleanly formed anti-Markovnikov product. In addition, it showed a different complex formation as indicated by the pyrrolic NH peak appearing around 10 ppm and shifted AB quartets similar to complex **1**; there is no peak in the negative region for possible formation of  $[\text{Mo}-\text{H}]$  species (see ESI, Fig. S18). Hence, complex **1** is the precatalyst and cleanly catalyzes at room temperature. It is likely that the mechanism could involve the decoordination of the pyrrole  $\pi$ -bond and the coordination of the incoming PhCCH followed by the nucleophilic attack of the secondary amine and protonolysis to give the product.

## Computational Studies

DFT calculations based on the hybrid exchange-correlation functional were performed to better understand the nature of bonding, the electronic structure and the conformations **LH**

**Figure 3.** Molecular orbital diagrams showing metal-pyrrole  $\pi$ -bonds for **1** and **2** (B3LYP/def2-SVP level).

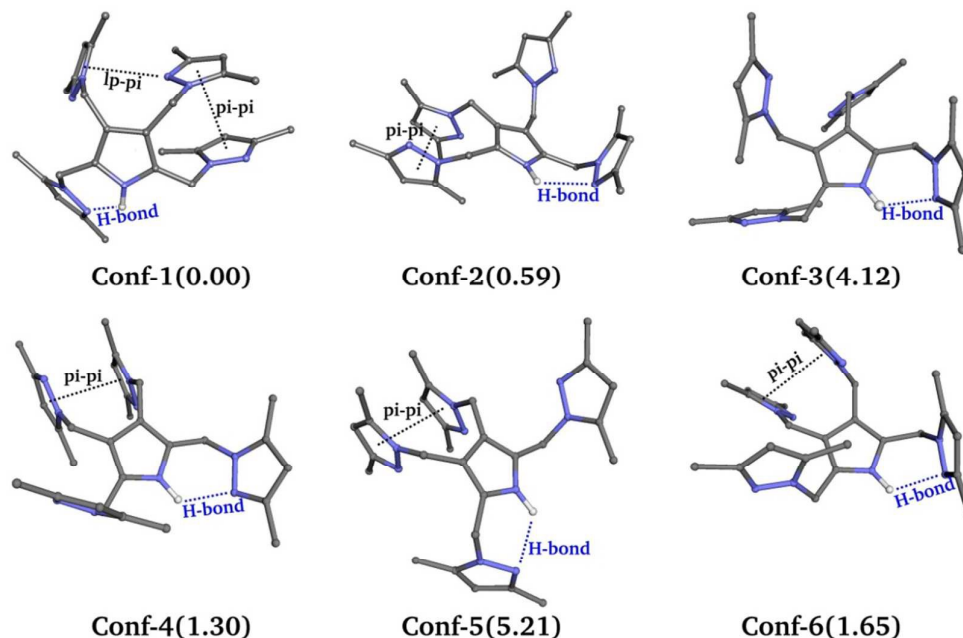


**Figure 4.** DFT (B3LYP/def2-SVP level) optimized six different possible conformations of LH based on the orientation of the pyrazolyl rings about the pyrrole ring plane. Their relative energies (kcal/mol) are given in parenthesis below each structure.

adopt in complex **1** and **2**. The geometry optimized structures are in close agreement with their X-ray structures. The HOMO–LUMO energy gap, calculated at B3LYP/def2-SVP level, is 3.72 eV and 3.52 eV for **1** and **2**, respectively. From the QTAIM analyses, the nature of bonding between the metal and the ligating atoms is described as coordinate bond as characterized by positive values for both the electron density ( $\rho(r_c) > 0$ ) and the Laplacian electron density ( $\nabla^2\rho(r_c) > 0$ ), and negative value of the Cremer–Kraka electron energy density ( $H(r_c) < 0$ ).<sup>37</sup> The bond strength estimations showed the M–C<sub>pyrrole</sub>  $\pi$  bonds are the weakest (for example, –39.5 and –45.5 kJ/mol for **1**) among the metal–ligand bonds in **1** and **2** and their Wiberg bond indices are 0.1736 (Mo–C<sub>4</sub>), 0.2079 (Mo–C<sub>5</sub>), 0.1758 (W–C<sub>4</sub>) and 0.2153 (W–C<sub>5</sub>), which are consistent with their relatively longer M–C<sub>pyrrole</sub> bond distances observed in their X-ray structures. However, the pyrrole ring C<sub>4</sub>–C<sub>5</sub> double bond distances found in the optimized structures of **1** (1.401 Å (B3LYP), 1.418 Å (BP86) and 1.398 Å (M06)) and **2** (1.404 Å (B3LYP), 1.421 Å (BP86) and 1.403 Å (M06)) are longer than the double bond distance 1.383 Å (B3LYP), 1.394 Å (BP86) and 1.376 Å (M06)) in the optimized free ligand structure conf-2 owing to coordination to the metal atoms. The MO diagrams corresponding to these pyrrole ring  $\pi$  interactions are shown in Figure 3.

The occupancies of the metal valence orbitals were analyzed using Natural Population Analysis (NPA) method (see ESI, Table T6). The Mo atom possesses 6.507 valence electrons with a natural partial charge of –1.11, and those for W atom are 6.697 and –0.68, respectively. The valence electronic configuration for Mo is 4d (6.12) and that for W is 5d (5.81). The d orbitals energy level ordering is consistent with the

simple crystal field theory model for an octahedral geometry with the  $t_{2g}$  set d orbitals being lower in energy than the  $e_g$  set orbitals. Among the  $t_{2g}$  orbitals, the occupancies of the  $d_{xy}$  and  $d_{yz}$  orbitals are higher than the  $d_{xz}$  orbital.

The extended charge decomposition analysis (ECDA) was performed to quantify the net amount of charge transferred between two fragments of the given complex (see ESI, Table T7). The theory of CDA is based on the molecular orbitals of complex composed by the linear combination of the donor and acceptor fragment orbitals (FO). The highest magnitude of net charge transfer (0.1519) was estimated for the carbonyl ligand (C<sub>3</sub>O<sub>3</sub>) lying trans to the pyrrole ring  $\pi$ -bond among the carbonyl ligands in complex **1**. Conversely, in the case of complex **2**, the highest net charge transfer 0.5286 was estimated for the carbonyl group (C<sub>2</sub>O<sub>2</sub>) lying trans to the pyrazolyl nitrogen atom, though they are isostructural. In addition, frequency calculations were performed, which closely match with the experimental  $\nu(\text{CO})$  values. The  $\nu(\text{CO})$  value decreases in the order C<sub>3</sub>O<sub>3</sub> > C<sub>1</sub>O<sub>1</sub> > C<sub>2</sub>O<sub>2</sub> and the higher value of  $\nu(\text{C}_3\text{O}_3)$  is due to its trans position to the coordinated pyrrole ring  $\pi$  bond which compete for backing bonding from the metal atom with CO.

### Conformations of LH

For the pyrrole molecule LH containing substituents in all  $\alpha$  and  $\beta$ -positions, the 3,5-dimethylpyrazolyl ring can lie above or below the pyrrole ring plane. The four pyrazolyl rings can be arranged in six different orientations about the pyrrole ring plane, giving the six different possible conformations

## ARTICLE

## Journal Name

represented as **conf-1** to **conf-6** and their optimized geometries are given in Figure 4. Their relative energy increases in the order, **conf-1** < **2** < **4** < **6** < **3** < **5**. Among these, **conf-1** possesses the lowest energy (0.00 kcal/mol) owing to the presence of the stabilizing  $\pi$ - $\pi$ , N- $\pi$  and H-bond interactions in the structure as indicated in Figure 4. The conformation **conf-5** has the highest energy (5.21 kcal/mol) as it exhibits less number of or weak stabilization interactions as compared to others. Interestingly, **conf-1**, **conf-2**, **conf-3** and **conf-5** have been observed in the X-ray structures of Pd(II), Ag(I) and Cu(I) complexes bearing **LH** reported previously.<sup>14</sup> Conformations **conf-4** and **conf-6** lie in the middle of the energy level ordering and were not observed to date. In complex **1** or **2**, **LH** adopts one of the lowest energy forms **conf-2**. Although metals could direct and bind with their own preferred conformations, it is interesting to investigate why the other two conformations have not been observed to date.

## Conclusions

The formation of two similar binuclear Mo(0) and W(0) carbonyl complexes presented here and the multinuclear complexes previously reported by us<sup>14</sup> show that the tetrakis(dimethylpyrazolylmethyl)pyrrole molecule is a versatile and flexible ligand for transition metal chemistry. To the best of our knowledge, the bridging mode of the pyrrole ring via  $\eta^2$ : $\eta^2$  hapticity found in these complexes is new and has not been reported to date. Although the  $\eta^2$  hapticity occupies one of the coordination sites of an octahedron, it is a weaker bond, as shown by the DFT calculations and can be labile. Interestingly, in contrast to the poor catalytic activity of of the binary carbonyl Mo(CO)<sub>6</sub>, the **LH** carbonyl complex **1** is the better catalyst precursor for the selective hydroaminations of phenylacetylene with a series of secondary amines. In most cases, the products are formed in excellent yields with a low catalyst loading at room temperature probably because of the multidentate nature of **LH** ligand which stabilizes the actual catalyst formed in situ and the catalysis reactions are selective. The energy of each possible conformations of **LH** based on the pyrazolyl ring orientations depends on the number of stabilizing interactions it possesses, as shown by DFT calculations. Other metal complexes of **LH** and their properties are under progress.

## Experimental Section

All reactions were carried out under nitrogen atmosphere using Schlenk line techniques or nitrogen-filled glove box. 2,3,4,5-Tetrakis(3,5-dimethylpyrazol-1-ylmethyl)pyrrole<sup>14</sup> and [W(CO)<sub>3</sub>(CH<sub>3</sub>CN)<sub>3</sub>]<sup>38</sup> were synthesized accordingly to the reported procedures. Other chemicals were obtained from commercial sources and used as received. Solvents were distilled before use by following the standard procedures. <sup>1</sup>H NMR (400 MHz or 600 MHz) and <sup>13</sup>C NMR (153.9 MHz) spectra were recorded at room temperatures. <sup>1</sup>H NMR and <sup>13</sup>C NMR chemical shifts were referenced with the chemical shift of the

residual protons present in the deuterated solvents. Chemical shifts are in parts per million, and coupling constants are in Hz. FTIR spectra were recorded using Perkin-Elmer Spectrum Rx. High Resolution Mass Spectra (ESI) were recorded using the Xevo G2 Tof mass spectrometer (Waters). GC-MS analyses were performed on a ThermoScientific TRACE 1300 system with ISQ mass detector and the capillary column of TG-5MS (30 m × 0.25 mm × 0.25  $\mu$ m, 5% phenyl methylpolysiloxane, 330/350 °C). The photolysis reaction was carried out using 125W medium pressure mercury lamp supplied by SAIC (India).  
**Synthesis of [Mo<sub>2</sub>(CO)<sub>6</sub>( $\mu$ - $\eta^2$ : $\eta^2$ -LH- $\kappa^4$ N)] **1****

**Method a:** A Schlenk flask equipped with water condenser was charged with Mo(CO)<sub>6</sub> (0.106 g, 0.40 mmol) and 2,3,4,5-tetrakis(3,5-dimethylpyrazol-1-ylmethyl)pyrrole (0.100 g, 0.20 mmol). To this was added THF (20 mL) and the resulting solution was refluxed for 36 h. The solution color changed to a dark brownish yellow. The resulting clear solution was cooled to room temperature, transferred to another Schlenk tube and then layered with petroleum ether. Yellow crystals of **1** were formed over a period of two weeks. The crystals were separated and dried under vacuum (0.093 g, 0.10 mmol). Yield: 50%. <sup>1</sup>H NMR(600 MHz, CDCl<sub>3</sub>):  $\delta$  = 9.26(br s, 1H, NH), 5.83(s, 2H, pyrazole CH), 5.76(s, 2H, pyrazole CH), 5.51(d, 2H, J(H<sub>A</sub>H<sub>B</sub>) = 15.2, CH<sub>2</sub>), 5.25(d, 2H, J(H<sub>A</sub>H<sub>B</sub>) = 15.2, CH<sub>2</sub>), 4.28(d, 2H, J(H<sub>A</sub>H<sub>B</sub>) = 14.4, CH<sub>2</sub>), 3.75(m, 4H, THF), 2.86(d, 2H, J(H<sub>A</sub>H<sub>B</sub>) = 14.0, CH<sub>2</sub>), 2.51(s, 6H, Me), 2.23(s, 6H, Me), 1.87(s, 6H, Me), 1.85(m, 4H, THF), 1.72(s, 6H, Me). <sup>13</sup>C{<sup>1</sup>H}NMR(153.9 MHz, CDCl<sub>3</sub>):  $\delta$  = 227.2(CO), 226.6(CO), 226.4(CO), 151.9(C<sub>3</sub> of Pz<sup>Me2</sup>), 151.6(C<sub>3</sub> of Pz<sup>Me2</sup>), 141.3(C<sub>5</sub> of Pz<sup>Me2</sup>), 139.8(C<sub>5</sub> of Pz<sup>Me2</sup>), 123.5( $\alpha$ -C of pyrrole ring), 107.1(CH of Pz<sup>Me2</sup>), 106.6(CH of Pz<sup>Me2</sup>), 104.8( $\beta$ -C of pyrrole ring), 68.0(THF), 46.8(CH<sub>2</sub>), 44.0(CH<sub>2</sub>), 25.8(THF), 16.5(Me of Pz<sup>Me2</sup>), 14.4(Me of Pz<sup>Me2</sup>), 12.0(Me of Pz<sup>Me2</sup>), 11.7(Me of Pz<sup>Me2</sup>). FTIR (KBr, cm<sup>-1</sup>):  $\nu$  = 3173(w), 3103(w), 2920(w), 1909(vs), 1793(vs), 1778(vs), 1552(m), 1463(m), 1437(m), 1385(w), 1372(w), 1291(w), 1262(w), 1090(w), 1045(m), 877(w), 802(m), 686(w), 658(w), 626(w), 594(w), 532(w), 515(w), 477(w). HRMS(+ESI): *m/z* calcd for [M + H<sup>+</sup>] C<sub>34</sub>H<sub>38</sub>Mo<sub>2</sub>N<sub>9</sub>O<sub>6</sub> 864.1048, found 864.1088.

**Method b:** A Schlenk flask equipped with water condenser was charged with 2,3,4,5-tetrakis(3,5-dimethylpyrazol-1-ylmethyl)pyrrole (0.050 g, 0.1 mmol) and Mo(CO)<sub>6</sub> (0.053 g, 0.2 mmol). THF (20 mL) was added and the solution was exposed to UV light ( $\lambda \geq 360$  nm) for 2h. The reaction mixture was transferred to another Schlenk tube and layered with petroleum ether. Yellow crystals of complex **1** were collected after 15 days and dried under vacuum (0.030 g, 0.03 mmol). Yield: 32%.

### Synthesis of [W<sub>2</sub>(CO)<sub>6</sub>( $\mu$ - $\eta^2$ : $\eta^2$ -LH- $\kappa^4$ N)] **2**

A Schlenk flask equipped with water condenser was charged with [W(CO)<sub>3</sub>(CH<sub>3</sub>CN)<sub>3</sub>] (0.110 g, 0.28 mmol) and 2,3,4,5-tetrakis(3,5-dimethylpyrazol-1-ylmethyl)pyrrole (0.070 g, 0.14 mmol). To this was added THF (20 mL) and the resulting solution was refluxed for 24 h. The solution color changed to a dark brownish yellow. The resulting clear solution was cooled to room temperature, transferred to another Schlenk tube and then layered with petroleum ether. Yellow crystals of **1** were

formed over a period of one month. The crystals were separated and dried under vacuum (0.030 g, 0.026 mmol). Yield: ~18%.  $^1\text{H NMR}(\text{CDCl}_3, 600 \text{ MHz}): \delta = 8.90(\text{br s}, 1\text{H}, \text{NH}),$

**Table 3.** Crystal Data and Structure Refinement for **1** and **2**.

	<b>1</b> ·THF	<b>2</b> ·1.5THF
Empirical formula	$\text{C}_{38}\text{H}_{45}\text{Mo}_2\text{N}_9\text{O}_7$	$\text{C}_{40}\text{H}_{49}\text{N}_9\text{O}_{7.5}\text{W}_2$
Formula weight	931.71	1143.58
Wavelength (Å)	0.71073	0.71073
Temperature (K)	100(2)	100(2)
Crystal system	Monoclinic	Monoclinic
Space group	<i>C2/c</i>	<i>C2/c</i>
<i>a</i> /Å	14.506(2)	14.4325(9)
<i>b</i> /Å	14.760(2)	14.7737(9)
<i>c</i> /Å	20.139(3)	20.2936(13)
$\alpha$ /degree	90.00	90.00
$\beta$ /degree	98.609(4)	99.005(2)
$\gamma$ /degree	90.00	90.00
Volume (Å <sup>3</sup> )	4263.3(12)	4273.7(5)
<i>Z</i>	4	4
$D_{\text{calcd}}, \text{g cm}^{-3}$	1.452	1.777
$\mu/\text{mm}^{-1}$	0.644	5.439
<i>F</i> (000)	1904	2240
$\theta$ range (degree)	1.980 to 25.000	1.985 to 24.999
Limiting indices	$-16 \leq h \leq 17, -17 \leq k \leq 17, -23 \leq l \leq 23$	$-17 \leq h \leq 16, -17 \leq k \leq 17, -21 \leq l \leq 24$
Total/ unique no. of reflns.	25081 / 3759	25049 / 3773
$R_{\text{int}}$	0.0485	0.0310
Data / restr./params.	3759 / 0 / 259	3773 / 0 / 259
GOF ( $F^2$ )	1.050	1.094
$R1, wR2$	0.0259, 0.0638	0.0209, 0.0514
<i>R</i> indices (all data) $R1, wR2$	0.0308, 0.0659	0.0229, 0.0524
Largest different peak and hole ( $e \text{ \AA}^{-3}$ )	0.459 and $-0.264$	1.091 and $-1.054$

5.81(s, 2H, pyrazole CH), 5.73(s, 2H, pyrazole CH), 5.41(d,  $J = 18.0$ , 2H,  $\text{CH}_2$ ), 5.33(d,  $J = 18.0$ , 2H,  $\text{CH}_2$ ), 4.29(d,  $J = 12.0$ , 2H,  $\text{CH}_2$ ), 3.75(m, 4H, THF  $\text{CH}_2$ ), 2.78(d,  $J = 12.0$ , 2H,  $\text{CH}_2$ ), 2.55(s, 6H,  $\text{CH}_3$ ), 2.23(s, 6H,  $\text{CH}_3$ ), 1.85(m, 4H, THF  $\text{CH}_2$ ), 1.82(s, 6H,  $\text{CH}_3$ ), 1.73(s, 6H,  $\text{CH}_3$ ).  $^{13}\text{C}\{^1\text{H}\}\text{NMR}(153.9 \text{ MHz}, \text{CDCl}_3): \delta = 222.0(\text{CO}), 220.0(\text{CO}), 219.4(\text{CO}), 152.6(\text{C}_3 \text{ of } \text{Pz}^{\text{Me}_2}), 151.5(\text{C}_3 \text{ of } \text{Pz}^{\text{Me}_2}), 141.2(\text{C}_5 \text{ of } \text{Pz}^{\text{Me}_2}), 139.9(\text{C}_5 \text{ of } \text{Pz}^{\text{Me}_2}), 119.6(\alpha\text{-C of pyrrole ring}), 107.1(\text{CH of } \text{Pz}^{\text{Me}_2}), 106.3(\text{CH of } \text{Pz}^{\text{Me}_2}), 100.3(\beta\text{-C of pyrrole ring}), 68.2(\text{THF}), 47.3(\text{CH}_2), 45.4(\text{CH}_2), 25.8(\text{THF}), 17.3(\text{Me of } \text{Pz}^{\text{Me}_2}), 14.6(\text{Me of } \text{Pz}^{\text{Me}_2}), 12.2(\text{Me of } \text{Pz}^{\text{Me}_2}), 12.0(\text{Me of } \text{Pz}^{\text{Me}_2}). \text{FT-IR (KBr, cm}^{-1}): \nu = 3422(\text{m}), 2925(\text{w}), 1899(\text{vs}), 1793(\text{vs}), 1773(\text{vs}), 1551(\text{m}), 1457(\text{m}), 1435(\text{m}), 1420(\text{m}), 1388(\text{m}), 1292(\text{w}), 1258(\text{w}), 1231(\text{w}), 1155(\text{w}), 1052(\text{w}), 1038(\text{w}), 873(\text{w}), 803(\text{w}), 581(\text{w}). \text{HRMS (+ESI): calcd } m/z \text{ for } [\text{M}-\text{H}^+] \text{C}_{34}\text{H}_{38}\text{W}_2\text{N}_9\text{O}_6: 1036.1958, \text{found: } 1036.2024.$

#### General Procedure for the Hydroamination Reactions

The typical procedure for the hydroamination reactions involves stirring the appropriate mixture consisting of phenylacetylene, amines and complex **1** taken in a Schlenk flask at room temperature or refluxed for the time period mentioned in Table 2. The volatiles were removed under vacuum to give the product, which was analyzed by  $^1\text{H NMR}$  and GCMS methods showing essentially the anti-Markovnikov product and compared with the literature spectra.<sup>35,39</sup>

#### X-ray Crystallography

Single crystal X-ray diffraction data collections for complex **1** and **2** were performed using Bruker-APEX-II CCD diffractometer with graphite monochromated Mo  $K\alpha$  radiation ( $\lambda = 0.71073 \text{ \AA}$ ). The space group for every structure was obtained by XPREP program. The structures were then solved by SIR-92<sup>40</sup> or SHELXS-97<sup>41</sup> available in WinGX, which successfully located most of the non-hydrogen atoms. Subsequently, least square refinements were carried out on  $F^2$  using SHELXL-2014 to locate the remaining non-hydrogen atoms. Non-hydrogen atoms were refined with anisotropic displacement parameters. All NH protons were located from the Difference Fourier Map. The displacement parameters of the NH hydrogen atoms were made dependent on the respective parent atom (1.2 times for the pyrrolic hydrogens). In the case of structure **2**·1.5THF, the unit cell contains one and half molecule of THF. This half THF molecule has been treated as a diffuse contribution to the overall scattering without specific atom positions by SQUEEZE/PLATON.<sup>42</sup> The refinement data for all the structures are summarized in Table 3.

#### Computational Details

The presented calculations are based on the density functional theory (DFT) formalism. The approach is based on the hybrid exchange-correlation functional proposed by Becke, Lee, Yang and Parr (B3LYP)<sup>43</sup> and the applied basis set is def2-SVP<sup>44</sup> including dispersion. In addition, density functionals BP86<sup>45</sup>

## ARTICLE

Journal Name

and M06<sup>46</sup> were also being used to compare the results with B3LYP functional. The minimum character of the stationary points obtained by geometry optimizations was checked by vibrational frequency calculations. Natural bond orbital (NBO) analysis was performed to explain the binding properties of complexes. The computed geometries were visualised using the GaussView 3.09 program and the computations were carried out using the GAUSSIAN 09 suite.<sup>47</sup> The wavefunction (.wfn) file obtained from gaussian-09 software was used as an input file to perform multiwfn program package for quantum theory atom in molecules (QTAIM).<sup>48</sup>

## Acknowledgements

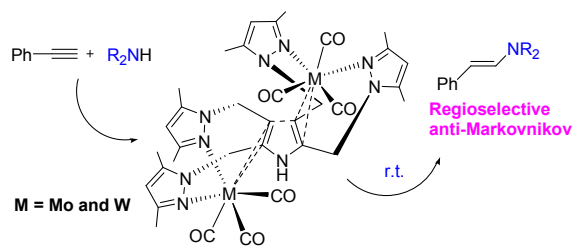
We thank the CSIR and DST (New Delhi, India) for financial support and for the X-ray, and NMR facilities. We thank Sanghamitra Das, Department of Chemistry, IIT-Kharagpur for recording a few NMR spectra.

## Notes and references

- (a) V. E. O. Fischer and W. Pfab, *Z. Naturforsch.* 1952, **7b**, 377; (b) G. Wilkinson, M. Rosenblum, M. C. Whiting and R. B. Woodward, *J. Am. Chem. Soc.* 1952, **74**, 2125.
- A. Almenningen, A. Haaland and J. Luszyk, *J. Organomet. Chem.* 1979, **170**, 271.
- G. Huttner, H. H. Brintzinger, L. G. Bell, P. Friedrich, V. Bejenke and D. Neugebauer, *J. Organomet. Chem.*, 1978, **145**, 329.
- E. O. Fischer and H. Wawersik, *J. Organomet. Chem.* 1966, **5**, 559.
- (a) M. O. Senge, *Angew. Chem. Int. Ed. Engl.* 1996, **35**, 1923; (b) K. Kowalski, *Coord. Chem. Rev.* 2010, **254**, 1895.
- (a) J. B. Love, P. A. Salyer, A. S. Bailey, C. Wilson, A. J. Blake, E. S. Davies and D. J. Evans, *Chem. Commun.* 2003, 1390; (b) D. L. Swartz II and A. L. Odom, *Dalton Trans.* 2008, 4254.
- (a) T. Dubé, S. Conoci, S. Gambarotta and G. P. A. Yap, *Organometallics*, 2000, **19**, 1182; (b) D. M. M. Freckmann, T. Dube, C. D. Berube, S. Gambarotta and G. P. A. Yap, *Organometallics*, 2002, **21**, 1240; (c) T. Dubé, S. Conoci, S. Gambarotta, G. P. A. Yap and G. Vasapollo, *Angew. Chem., Int. Ed.* 1999, **38**, 3657; (d) M. Ganesan, S. Gambarotta and G. P. A. Yap, *Angew. Chem., Int. Ed.* 2001, **40**, 766; (e) M. Ganesan, C. D. Berube, S. Gambarotta and G. P. A. Yap, *Organometallics*, 2002, **21**, 1707.
- (a) K. K. Joshi, P. L. Pauson, A. R. Qazi and W. H. Stubbs, *J. Organomet. Chem.* 1964, **1**, 471; (b) R. B. King and M. B. Bisnette, *Inorg. Chem.* 1964, **3**, 796.
- (a) N. Kuhn, M. Köckerling, S. Stubenrauch, D. Bläser and R. Boese, *J. Chem. Soc., Chem. Commun.* 1991, 1368; (b) M. Kreye, D. Baabe, P. Schweyen, M. Freytag, C. G. Daniliuc, P. G. Jones and M. D. Walter, *Organometallics*, 2013, **32**, 5887; (c) H. Schumann, J. Gottfriedsen and J. Demtschuk, *Chem. Commun.* 1999, 2091.
- (a) H. Schumann, E. C. E. Rosenthal, J. Winterfeld, G. Kociok-Koehn, *J. Organomet. Chem.* 1995, **495**, C12; (b) N. Kuhn, S. Stubenrauch, R. Boese and D. Bläser, *J. Organomet. Chem.* 1992, **440**, 289.
- M. Kreye, M. Freytag, C. G. Daniliuc, P. G. Jones, and M. D. Walter, *Z. Anorg. Allg. Chem.* 2015, **641**, 2109.
- (a) K. Yünlü, F. Basolo, A. L. Rheingold, *J. Organomet. Chem.*, 1987, **330**, 221; (b) M. Westerhausen, M. Wieneke, H. Nöth, T. Seifert, A. Pfitzner, W. Schwarz, O. Schwarz, and J. Weidlein, *Eur. J. Inorg. Chem.* 1998, 1175.
- S. D. Angelis, E. Solari, C. Floriani, A. Chiesi-Villa and C. Rizzoli, *J. Chem. Soc. Dalton Trans.* 1994, 2467.
- D. Ghorai and G. Mani, *Inorg. Chem.*, 2014, **53**, 4117.
- S. Trofimenko, *J. Chem. Edu.* 2005, **82**, 1715.
- D. Ulku, M. N. Tahir and S. Ozkar, *Acta. Cryst.* 1997, **C53**, 185.
- D. Ghorai, S. Kumar, G. Mani, *Dalton Trans.* 2012, **41**, 9503.
- B. Cordero, V. Gómez, A. E. Platero-Prats, M. Revés, J. Echeverría, E. Cremades, F. Barragán and S. Alvarez, *Dalton Trans.*, 2008, 2832.
- D. J. Wink and C. Kyeong Oh, *Organometallics*, 1990, **9**, 2403.
- W. W. Seidel, M. Schaffrath and T. Pape, *Angew. Chem., Int. Ed.* 2005, **44**, 7798.
- F.-W. Grevels, J. Jacke, P. Betz, C. Kruger and Y.-H. Tsay, *Organometallics*, 1989, **8**, 293.
- M. Górski, A. Kochel and T. Szymańska-Buzar, *Organometallics*, 2004, **23**, 3037.
- T. E. Müller and M. Beller, *Chem. Rev.* 1998, **98**, 675.
- F. Pohlki and S. Doye, *Chem. Soc. Rev.* 2003, **32**, 104.
- F. Alonso, I. P. Beletskaya and M. Yus, *Chem. Rev.* 2004, **104**, 3079.
- T. E. Müller, K. C. Hultzs, M. Yus, F. Foubelo and M. Tada, *Chem. Rev.* 2008, **108**, 3795.
- L. Huang, M. Arndt, K. Gooßen, H. Heydt and L. J. Gooßen, *Chem. Rev.* 2015, **115**, 2596.
- A. R. Shaffer and J. A. R. Schmidt, *Organometallics*, 2008, **27**, 1259.
- V. Lavallo, G. D. Frey, B. Donnadiou, M. Soleilhavoup, and G. Bertrand, *Angew. Chem., Int. Ed.* 2008, **47**, 5224.
- L. Wang, L. Kong, Y. Li, R. Ganguly and R. Kinjo, *Chem. Commun.*, 2015, **51**, 12419.
- Michael, F. E.; Cochran, B. M. *J. Am. Chem. Soc.* 2006, **128**, 4246.
- S. M. Bronner and R. H. Grubbs, *Chem. Sci.* 2014, **5**, 101.
- K. D. Hesp and M. Stradiotto, *ChemCatChem*, 2010, **2**, 1192.
- F. E. McDonald and A. K. Chatterjee, *Tetrahedron Lett.* 1997, **38**, 7687.
- P. Kociecka, I. Czelusniak and T. Szymanska-Buzar, *Adv. Synth. Catal.* 2014, **356**, 3319.

36. 1-Dodecanol was used as an internal standard for calculating the yield by GCMS.
37. (a) R. F. W. Bader and H. Essen, *J. Chem. Phys.*, 1984, **80**, 1943; (b) D. Cremer and E. C. Kraka, *Chem. Acta*, 1984, **57**, 1259.
38. D. P. Tate, W. R. Knipple and J. M. Augl, *Inorg. Chem.* 1962, **1**, 433.
39. G. Bélanger, M. Doré, F. Ménard and V. Darsigny, *J. Org. Chem.* 2006, **71**, 7481.
40. A. Altomare, G. Cascarano, C. Giacovazzo and A. Guagliardi, *J. Appl. Cryst.*, 1993, **26**, 343.
41. G. M. Sheldrick, *Acta Crystallogr.*, 2008, **A64**, 112.
42. P. van der Sluis and A. L. Spek, *Acta Cryst. A* 1990, **46**, 194.
43. C. Lee, W. Yang and R. G. Parr, *Phys. Rev. B* 1988, **37**, 785.
44. A. Schaefer, H. Horn and R. Ahlrichs, *J. Chem. Phys.* 1992, **97**, 2571.
45. (a) J. P. Perdew, *Phys. Rev. B: Condens. Matter Mater. Phys.* 1986, **33**, 8822. (b) A. D. Becke, *Phys. Rev. A: At., Mol., Opt. Phys.* 1988, **38**, 3098.
46. (a) Y. Zhao, D. G. Truhlar, *J. Chem. Phys.* 2006, **125**, 194101. (b) Y. Zhao, D. G. Truhlar, *Theor. Chem. Acc.* 2008, **120**, 215.
47. M. J. Frisch, et. al. Gaussian 09, Revision C.01; Gaussian, Inc.: Wallingford, CT, 2010.
48. T. Lu and F. W. Chen, *J. Comput. Chem.* 2012, **33**, 580.

For Table of Contents



The new pyrrole ring  $\pi$ -bonds bridged binuclear Mo complex catalyzes the regioselective hydroamination of phenylacetylene with a series of secondary amines at room temperature giving the products in very high yields.